OPEN

Multimodal Device and Computer Algorithm–Based Monitoring of Pancreatic Microcirculation Profiles In Vivo

Yuan Li, MD, Xiaohong Song, MD,* Mingming Liu, PhD,*† Bing Wang, PhD,* Jian Zhang, MD,*† Ailing Li, PhD,* Honggang Zhang, MD,* and Ruijuan Xiu, PhD**

Objectives: Pancreatic microcirculation has an essential role in orchestrating pancreatic homeostasis. Inherent complexity and technological limitation lead to interobserver variability and 1-sided microcirculatory data. Here, we introduce a multimodal device and computer algorithm–based platform for monitoring and visualizing integrated pancreatic microcirculation profiles.

Methods: After anesthetizing and exposing pancreas tissue of BALB/c mice, probes of Oxygen to See, Microx TX3, and MoorVMS-LDF2 were positioned at pancreas in situ to capture the pancreatic microcirculatory oxygen (hemoglobin oxygen saturation, relative amount of hemoglobin, and partial oxygen pressure) and microhemodynamic data (microvascular blood perfusion and velocity). To assess and visualize pancreatic microcirculation profiles, raw data of pancreatic microcirculation profiles were processed and transformed using interquartile range and min-max normalization by Python and Apache ECharts.

Results: The multimodal device–based platform was established and 3-dimensional microcirculatory modules were constructed. Raw data sets of pancreatic microcirculatory oxygen and microhemodynamic were collected. The outlier of data set was adjusted to the boundary value and raw data set was preprocessed. Normalized pancreatic microcirculation profiles were integrated into the 3-dimensional histogram and scatter modules, respectively. The 3-dimensional modules of pancreatic microcirculation profiles were then generated.

Conclusions: We established a multimodal device and computer algorithm–based monitoring platform for visualizing integrated pancreatic microcirculation profiles.

Key Words: pancreatic microcirculation profiles, hemoglobin oxygen saturation, relative amount of hemoglobin, partial oxygen pressure, blood perfusion

From the *Institute of Microcirculation, Chinese Academy of Medical Sciences & Peking Union Medical College; and †Diabetes Research Center, Chinese Academy of Medical Sciences & Peking Union Medical College, Beijing, China.

Received for publication January 8, 2020; accepted June 23, 2020.

Y.L. and X.H.S. contributed equally to this study.

Address correspondence to: Mingming Liu, PhD or Honggang Zhang, MD, Institute of Microcirculation, Chinese Academy of Medical Sciences & Peking Union Medical College (CAMS & PUMC), No. 5 Dong Dan San Tiao, Dongcheng District, Beijing, 100005, China (e-mail: mingmingliu@imc.pumc.edu.cn; zhanghg1966126@163.com).

This study was supported by grants from the CAMS Initiative for Innovative Medicine (CAMS-I2M, No. 2016-I2M-3-006) and the National Natural Science Foundation of China (No. 81900747).

The authors declare no conflict of interest.

Supplemental digital contents are available for this article. Direct URL citations appear in the printed text and are provided in the HTML and PDF versions of this article on the journal's Web site (www.pancreasjournal.com).

DOI: 10.1097/MPA.0000000000001627

Abbreviations: 3-D - 3-dimensional, IQR - interquartile range, PO_2 - partial oxygen pressure, PU - perfusion unit, rHb - relative amount of hemoglobin, SO_2 - hemoglobin oxygen saturation

(*Pancreas* 2020;49: 1075–1082)

Microcirculation refers to the blood flow in vessels less than 150 μm in diameter, including arterioles, capillaries, and venules, which is pivotal for regulating tissue homeostasis. Tasked with transporting oxygen and nutrients, microcirculation profiles include both microcirculatory oxygen and microhemodynamic consortia. Therefore, characterization of complex microcirculation profiles gives a better understanding of the role that microcirculation plays in pathogenesis, development, and even prevention of diseases.

Pancreatic microcirculatory milieu, mainly composed of pancreatic microvascular endothelial cells, has an essential role in orchestrating adjustment of pancreatic homeostasis to match local tissue blood perfusion with metabolic demand and preserve pancreatic physiological function. Microcirculatory maladjustment may lead to inadequate nutrients and oxygen supply, which results in consequential pancreatic dysfunction.[1] Emerging evidence confirms that pancreatic microcirculation profiles may serve as a determinant for variety of pathological conditions such as diabetes,[2] acute pancreatitis,[3,4] pancreatic cancer,[5,6] even hypertension, and obesity.[7] Therefore, the pancreatic microcirculation may herald, either as a marker or as a possible mechanism, the development of pancreatic-related diseases.

In our previous report, we analyzed the functional status of pancreatic microcirculation depending on microhemodynamic data. However, as an interconnected microcirculatory system, microhemodynamic variables, and microcirculatory oxygen parameters are both considered as the key determinants of the exchange of substances between microcirculation and tissues. Meanwhile, Premont et al[8] confirmed that continuous supplement of oxygen in microvasculature was central to the maintenance of normal physiological status and metabolic demand. Therefore, the scenario is not intact only by observing and analyzing microcirculatory hemodynamic data. The microcirculatory oxygen characteristics also provide crucial information for microcirculation profiles with comprehensive level, which further improves the progress in investigating microcirculatory pathogenesis for pancreatic-related diseases. In this respect, concerted efforts to establish "pancreatic microcirculatory observatories" to promote progress are needed.

Traditionally, studies of the microcirculation generally focused on microvascular blood perfusion. Recently, techniques have evolved and improved assessment of microcirculatory oxygen parameters (such as hemoglobin oxygen saturation [SO_2], the relative amount of hemoglobin [rHb] in the microvessels, and partial oxygen pressure [PO_2] in vivo). Here, we described a multimodal device and computer algorithm–based platform for comprehensive assessment of pancreatic microcirculation profiles in visualized 3-dimensional (3-D) modules.

MATERIALS AND METHODS

Animals

This study was approved by the Institutional Animal Care and Use Committee at the Institute of Microcirculation, Chinese Academy of Medical Sciences (CAMS). All mice were cared humanely, and all experiments were performed in compliance with the guidelines and regulations. Eight-week-old male BALB/c mice (n = 6, 25–30 g) were provided by the Institute of Laboratory Animal Sciences (CAMS, Beijing, China) and were kept in the animal facility under a specific-pathogen-free condition. Mice were housed separately in the cages of the animal room (temperature, 26°C; humidity, 55%–70%) under a 12-hour light/dark cycle and were fed with standard laboratory diet and water ad libitum.

Setup of a Multimodal Device–Based Microcirculatory Monitoring Platform

To determine pancreatic microcirculation profiles, the Oxygen to See (O2C; LEA Medizintechnik GmbH, Giessen, Germany), Microx TX3 (PreSens; Precision Sensing GmbH, Regensburg, Germany), and a dual-channel laser Doppler monitoring instrument (VMS-LDF2; Moor Instrument, Ltd, Axminster, United Kingdom) were used to configure the multimodal device (Fig. 1). The multimodal device contained white light (wavelengths of 500–800 nm) and laser (wavelengths of 785 nm), which was used to capture the microcirculatory oxygen and microhemodynamic data of the pancreas tissue. The probes allowed scattered light to spread out through the pancreas tissue in a diffuse pattern. Based on the principle that a part of light spectrum is absorbed when the white light interacts with the erythrocytes, the O2C, equipped with white light spectroscopy, allowed the determination of So_2 and rHb. The principle of the Microx TX3 is based on the light quenching of fluorescence caused by the collision of oxygen molecules and oxygen-sensitive fluorescence materials. Therefore, the Microx TX3 could measure Po_2 with the photochemical oxygen sensor, which includes a polymer fiber and an oxygen optical sensor. Furthermore, the VMS-LDF2 enabled the determination of pancreatic microvascular blood perfusion and blood flow velocity.

Animal Surgical Preparation

All mice were acclimatized for 30 minutes in a thermostatic laboratory at 26.0°C (standard deviation [SD], 0.5). After anesthetizing with 2% inhaled isoflurane (R510-22; RWD Life Science Co, Ltd, Shenzhen, China) in a 50% mixture of oxygen using small animal anesthesia machine (Matrx VMR; Midmark Corporation, Dayton, Ohio), mice were fixed on the operating plank in supine position with continued inhalation of volatile gas isoflurane. A designed 10-mm incision along the midline of the upper abdomen was made to expose the pancreas tissue and a stereotaxic holder was used to position and advance the probes within 1 mm upon the exposed pancreas tissue steadily. The temperature of pancreas tissue was monitored continuously to make sure it remained constant in the duration of the experiments.

Determination of Microcirculatory Oxygen of Pancreatic Microcirculation

Microcirculatory oxygen of pancreatic microcirculation profiles include the So_2, rHb, and Po_2. The LF-2 probe of O2C was guided to the exposed pancreas tissue. Because the sampled volume of tissue is considered to be approximately a depth of half the probe spacing,[9] the thickness of measured pancreas was approximately 1 mm in our method. The detected So_2 is a measure of mean So_2 across arterioles, capillaries, and venules in the microvasculature, whereas rHb represents the rHb in pancreatic microcirculation. Meanwhile, Po_2 of pancreas tissue was measured using the Microx TX3 based on the oxygen-dependent quenching of fluorescent material after colliding with oxygen molecule.

Microcirculatory Hemodynamics of Pancreatic Microcirculation Profiles

Pancreatic microhemodynamic data, including microvascular blood perfusion and velocity, were captured by a dual-channel laser Doppler monitoring system (Moor Instrument) with a 785-nm VP4 probe as previously described. Briefly, after anesthetizing, the VP4 electrode was fixed and advanced within 1 mm of the exposed pancreas tissue. The probe was repositioned after each measure to avoid additive effects and localized exhaustion of contraction and relaxation ability. The raw data of blood perfusion and velocity of pancreatic microcirculation were collected.

Construction of 3-D Module of Pancreatic Microcirculation Profiles

We aimed to establish the 3-D module that characterizes pancreatic microcirculation reflecting variability of the functional status of microcirculation. To achieve this, the 3-D module of pancreatic microcirculation profiles was generated, descripted, and visualized by using Python (Version 3.7.4, https://www.python.org/) and Apache ECharts (Released Version 4.2.0-rc.2, https://echarts.apache.org) tool licensed under the Apache License, Version 2.0 (http://www.apache.org/licenses/LICENSE-2.0) with demo microcirculatory data set (please see Supplemental Digital Content 1, http://links.lww.com/MPA/A807). In demo 3-D module, the time course, microcirculatory variables, and calculated value of demo oxygen and microhemodynamic data were

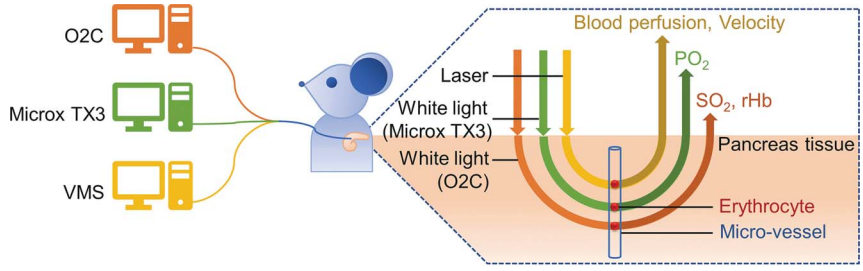

FIGURE 1. Schematic of multimodal device and computer algorithm–based pancreatic microcirculation profiles monitoring platform. The probes of the O2C, Microx TX3, and the dual-channel laser Doppler VMS were used to determine the pancreatic microcirculatory oxygen and microhemodynamic data sets. The white light was scattered and returned to the detectors of the O2C and Microx TX3. Depending on the Doppler principle, the pancreatic microvascular perfusion signals were captured. With the microcirculatory monitoring platform, So_2, rHb, Po_2, blood perfusion, and velocity of pancreatic microcirculatory profiles could be obtained.

defined as the *X*, *Y*, and *Z* axis, respectively. Then, the pancreatic microcirculatory oxygen and microhemodynamic data sets captured from multimodal device were preprocessed and analyzed by Python. In addition, the comprehensive pancreatic microcirculation profiles were adjusted and visualized in a single 3-D dynamic microcirculatory module, superposing detected So_2, rHb, Po_2, blood perfusion, and velocity of pancreatic microcirculation. Because of the difference of sampling frequency and parameter setting among multimodal device, outlier processing and microcirculatory data set integrating were performed.

Outlier Processing

To generate an automated data preprocessing, the identification and adjustment of outliers were considered in our algorithm. Box plots algorithm was used in the script to automatically exclude the outlier. We defined Q_1 as the 25th percentile largest value and Q_3 as the 75th percentile largest value. Interquartile range (IQR) was defined as the difference between Q_3 and Q_1. Under this concept, the range from $(Q_1 - 3 \times IQR)$ to $(Q_3 + 3 \times IQR)$ was considered the boundary of microcirculatory values, and the microcirculatory data exceeding this boundary were taken as outliers and would be adjusted to the nearest boundary value. All microcirculatory data processed by IQR method could be scaled to the interval of the module, and more than 95% of the data were classified as validation.

Integration of Pancreatic Microcirculatory Dataset

Considering that the units of data sets in the pancreatic microcirculation profiles were different, we standardized the pancreatic microcirculatory data set to visualize and to optimize the integrated pancreatic microcirculation profiles in a single coordinate. The min-max normalization and the relative value normalization were 2 commonly mathematical converting algorithms for removing the limitation derived from data set dimension,[10] which allowed divergence of variables with different units displayed in a single coordinate. Therefore, these 2 normalized algorithms were used to adjust the dimension of the 3-D module.

The min-max normalization is calculated as follows:

$$x' = \frac{x - \min}{\max - \min} \quad (1)$$

where x represents the raw data of pancreatic microcirculation data set. x' is the normalized data after normalization. Min value represents the minimum value of the microhemodynamic and microcirculatory oxygen data and max value represents the maximum value. Furthermore, considering the time granularity of data set was divergent, the microhemodynamic and oxygen data sets of pancreatic microcirculation were transformed by least common multiple method, so that it could be integrated in the single 3-D module. The microcirculatory data were then unified in the range of [0, 1], which maintained their original characteristics through these mathematically adjustment.

The relative value normalization is calculated as follows:

$$x' = \frac{x}{\mathrm{Me}} \quad (2)$$

where x represents the raw data of pancreatic microcirculatory data set. Me represents the median value of the microcirculatory oxygen and microhemodynamic data, whereas x' represents the normalized value.

RESULTS

Construction of 3-D Microcirculatory Modules

Our goal was to develop a multimodal device–based platform to monitor and visualize the integrated pancreatic microcirculation profiles. Thus, a demo data set was generated randomly that contained demo microcirculatory oxygen and microhemodynamic data sets (please see Supplemental Digital Content 1, http://links.lww.com/MPA/A807). The schematics of constructed microcirculatory 3-D modules were illustrated in Figure 2 and Figure 3. Three-dimensional histogram was applied to show the dynamic tendency of microcirculatory parameters (Fig. 2), and 3-D scatter plot was used to show distribution of microcirculatory data set (Fig. 3), respectively. In the 3-D histogram, the demo data set, including So_2, rHb, and microvascular blood perfusion (Figs. 2A–C), was used to illustrate the construction framework. Meanwhile, the perspectives of the front view (Fig. 2D), side view (Fig. 2E), and overlook view (Fig. 2F) were generated and rotated based on the established 3-D module in ECharts. Similarly, in the 3-D scatter plot, the distribution of each demo data set was shown in Figures 3A to C, and the front view (Fig. 3D), side view (Fig. 3E), and overlook view (Fig. 3F) were illustrated in the lower panel. Furthermore, the established demo 3-D histogram and 3-D scatter modules were recorded as videos to display the dynamic exhibiting function of zooming in, zooming out, and rotation (please see Supplemental Video 1, http://links.lww.com/MPA/A810, Supplemental Video 2, http://links.lww.com/MPA/A811, and Supplemental Legends, http://links.lww.com/MPA/A808).

Raw Data of Pancreatic Microcirculation Profiles

The established multimodal device–based microcirculatory monitoring platform enabled us to characterize the integrated pancreatic microcirculation profiles in vivo comprehensively and dynamically. The raw data of pancreatic microcirculatory oxygen were illustrated in Figure 4. The So_2 illustrated the distribution of So_2 in pancreatic microcirculation, which reached 93.43% (SD, 3.28; Fig. 4A). The amount of hemoglobin in pancreatic microcirculation was quantified by rHb, whose baseline was 68.72 AU (SD, 6.09; Fig. 4B). The baseline of pancreatic microcirculatory Po_2 was 59.71 hPa (SD, 5.84; Fig. 4C). Given that microcirculatory blood perfusion is one of the important factors of microcirculation profiles, we captured raw data of pancreatic microhemodynamic including blood perfusion and velocity by vascular monitoring system (VMS). Generally, microvascular vasodilation and vasoconstriction were observed in all mice (Fig. 4D). Representative pancreatic microcirculatory blood perfusion (5 seconds) extracted from microvascular blood perfusion was shown in Figure 4E. The pancreatic blood distribution pattern was illustrated in Figure 4F. Velocity of microcirculatory blood perfusion was shown in Figure 4G. In contrast to microcirculatory oxygen data set, as expected, microhemodynamics was more rhythmical. Taken together, these raw pancreatic microcirculatory oxygen and microhemodynamic data sets led to a description of integrated microcirculation profiles, which revealed the dynamic differential status of microcirculation.

Three-Dimensional Modules of Pancreatic Microcirculation Profiles

Next, to develop the 3-D module that characterizes integrated pancreatic microcirculation profiles, according to the original coordinate axis, the raw pancreatic oxygen and microhemodynamic data sets were preprocessed by the steps mentioned in the Materials

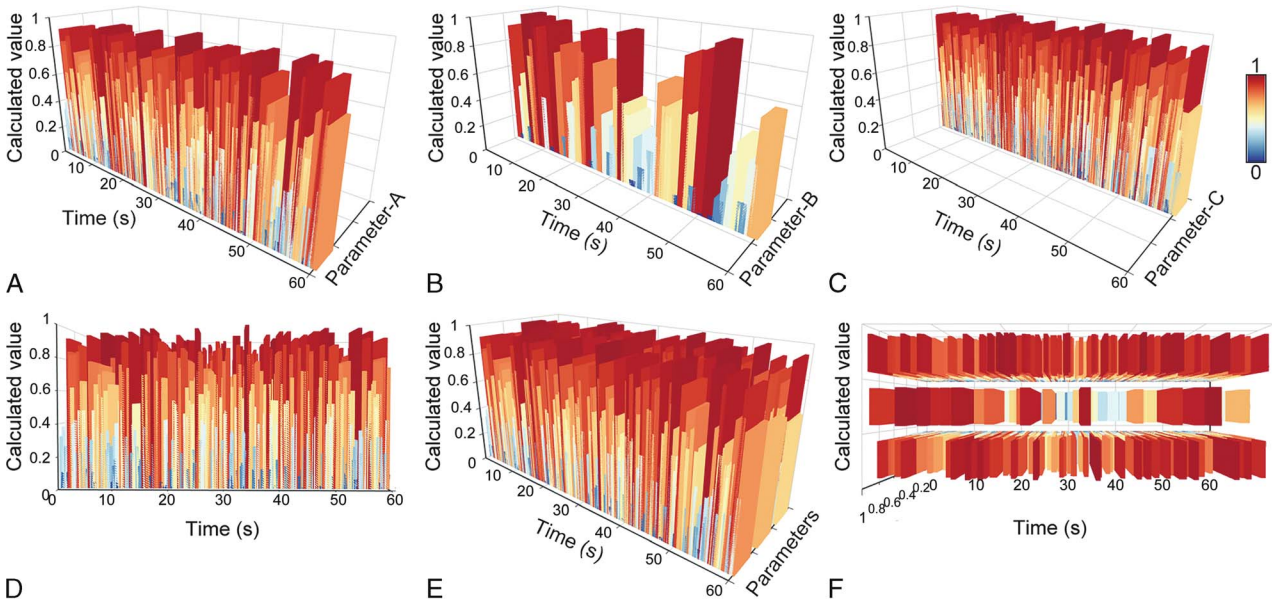

FIGURE 2. Outline of the construction workflow of 3-D module with demo microcirculatory data set. A–C, Demo microcirculatory oxygen and microhemodynamic data sets located in the coordinates. D–F, Separated demo microcirculatory data were integrated into a single coordinate. The front, side, and overlook views were generated by rotation. The front view was shown in D. Although the side view in E was rotated 45 degrees toward left. The overlook view in F was rotated 90 degrees toward down. Details of demo microcirculatory data set used in construction of 3-D module were attached in Supplemental Digital Content 1, http://links.lww.com/MPA/A807.

and Methods section. The pancreatic microcirculatory data set was reconstructed in the established 3-D module. The superposed So_2, rHb, Po_2, blood perfusion, and velocity of pancreatic microcirculation were comprehended, which could be visualized as an integrity profile. The time course, pancreatic microcirculatory parameters, and calculated values were defined as the *X*, *Y*, and *Z* axis of the 3-D module, respectively. Meanwhile, the normalized values of pancreatic microcirculatory oxygen and microhemodynamic were integrated in the modules (Figs. 5A–E, 6A–E). The perspectives of front view (Figs. 5F, 6F), side view (Figs. 5G, 6G), and overlook view (Figs. 5H, 6H) were rotated. In addition, the dynamic scenarios of both established 3-D modules of integrated pancreatic microcirculation profiles were provided (please see Supplemental Video 3, http://links.lww.com/MPA/A812, Supplemental Video 4, http://

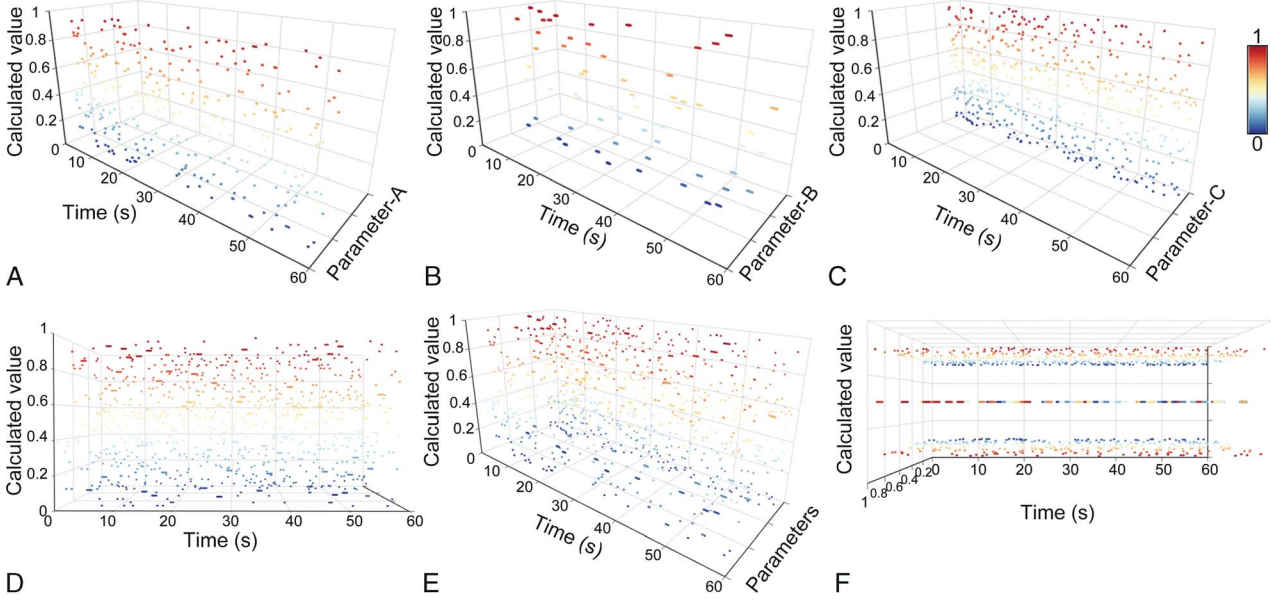

FIGURE 3. The framework of construction of 3-D distribution module. A–C, Single distribution plot was constructed and set into coordinate using demo oxygen and microhemodynamic data sets. D–F, Separated microcirculatory oxygen and microhemodynamic demo data sets were integrated into a single coordinate. The front (D), side (E), and overlook views (F) were generated by rotation. The side view of distribution module in E was rotated 45 degrees toward left and the overlook view in F was rotated 90 degrees toward down.

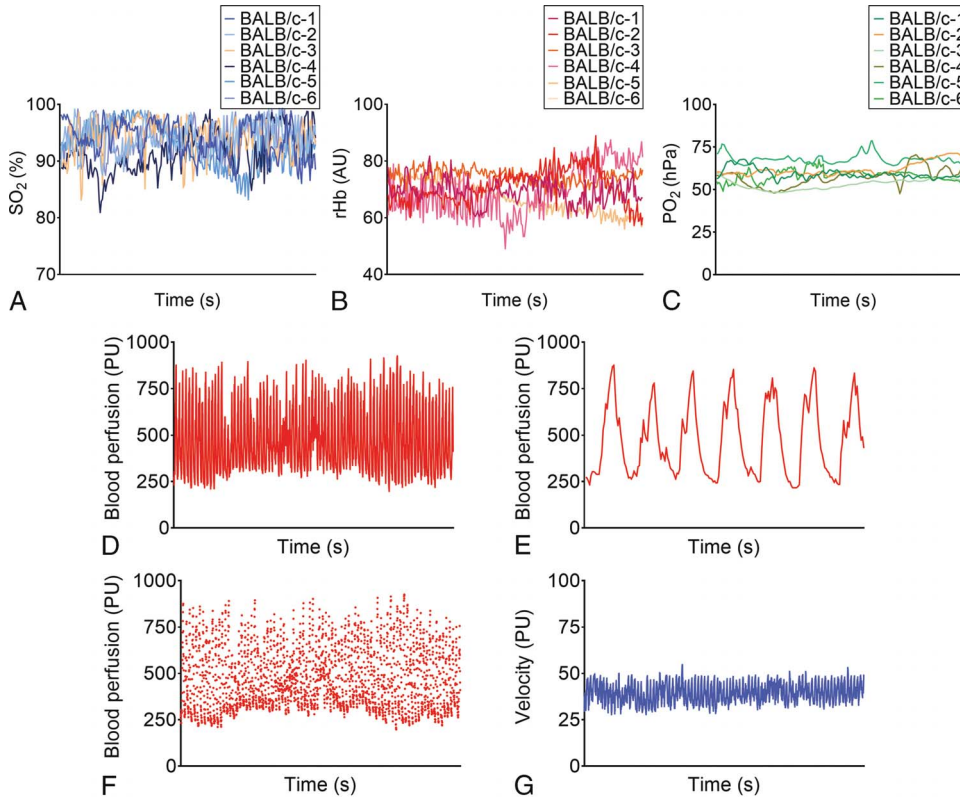

FIGURE 4. Raw pancreatic microcirculatory oxygen and microhemodynamic data. A–C, The So_2 (A), rHb (B), and Po_2 (C) of pancreatic microcirculation were obtained by the O2C and Microx TX3. D–G, Representative blood perfusion and velocity of pancreatic microcirculation were captured by the VMS. D, Pancreatic microcirculatory blood perfusion. E, Representative pancreatic microcirculatory blood perfusion (5 seconds) extracted from microvascular blood perfusion data set. F, Distribution pattern of pancreatic microcirculation profiles. G, Velocity of the pancreatic blood flow. PU indicates perfusion unit.

links.lww.com/MPA/A813, and Supplemental Legends, http://links.lww.com/MPA/A808).

As for the microcirculatory oxygen and microhemodynamic data sets, it was noted that the ranges of microcirculatory values processed by relative value normalization algorithm would exceed the [0, 1] range, especially microhemodynamic data set. In addition, because all data were compared with the median of corresponding data set in the relative value normalization algorithm, the differences among global calculated data were consequently reduced, which lost the intrinsic characteristic of pancreatic microcirculatory data set in some extent. The min-max normalization algorithm was better than the relative value normalization algorithm, which could preserve the original characteristic of pancreatic microcirculation profiles (please see Supplemental Fig. 1, http://links.lww.com/MPA/A809). After adjustment, the microcirculation profiles complied the 3-D modules well.

DISCUSSION

Our current study is the first method to report a multimodal device and computer algorithm–based 3-D visualization of integrated pancreatic microcirculation profiles. Pancreatic microcirculation is a system composed of interconnected microvessels, which is responsible for the distribution of oxygenated blood flow within pancreas tissue according to regional metabolic demand. Because heterogeneity (different organs exhibit discrepant microcirculation profiles) and variability (the microcirculation profiles are affected by multiple relevant factors) of microcirculation, early attempts at visualized microcirculation have struggled for decades to make accurate modules exhibiting the inherent properties of microcirculation profiles. Considering the characteristic and integrity of pancreatic microcirculation profiles including microcirculatory oxygen and microhemodynamic data, we proposed 3-D modules for visualizing pancreatic microcirculation profiles, thereby meeting the expectations for future development of microcirculation assessment in experimental and clinical individuals. The proposed multimodal device and algorithm-based platform enable exhibiting blood perfusion-oxygen diagram globally via 3-D dynamic modules.

Structurally, the pancreas is a complex highly vascularized gland, which possesses a higher basal and stimulated blood flow. Each pancreatic β-cell is in contact with a capillary to allow sensing of blood glucose and the subsequent hormone secretion. In addition to transporting nutrient and oxygen, pancreatic microvasculature is required for physiological function. Earlier studies used invasive methods to assess microvascular function, such as traditionally scanning electron microscopy of microcorrosion casts,[11] catheterization-based techniques, or less invasive positron emission tomography, which led to inaccurate microcirculatory data. Our multimodal device–based platform provides relative noninvasive, accessible, and accurate measurements of pancreatic microcirculatory oxygen. The pancreatic microcirculatory oxygen profiles captured and visualized by our method include So_2, rHb, and Po_2, which are fundamental descriptors of pancreatic microcirculation profiles. Although separated oxygen parameters such as blood So_2 could be measured by near infrared spectroscopy,[12] incorporated within the O2C and Microx

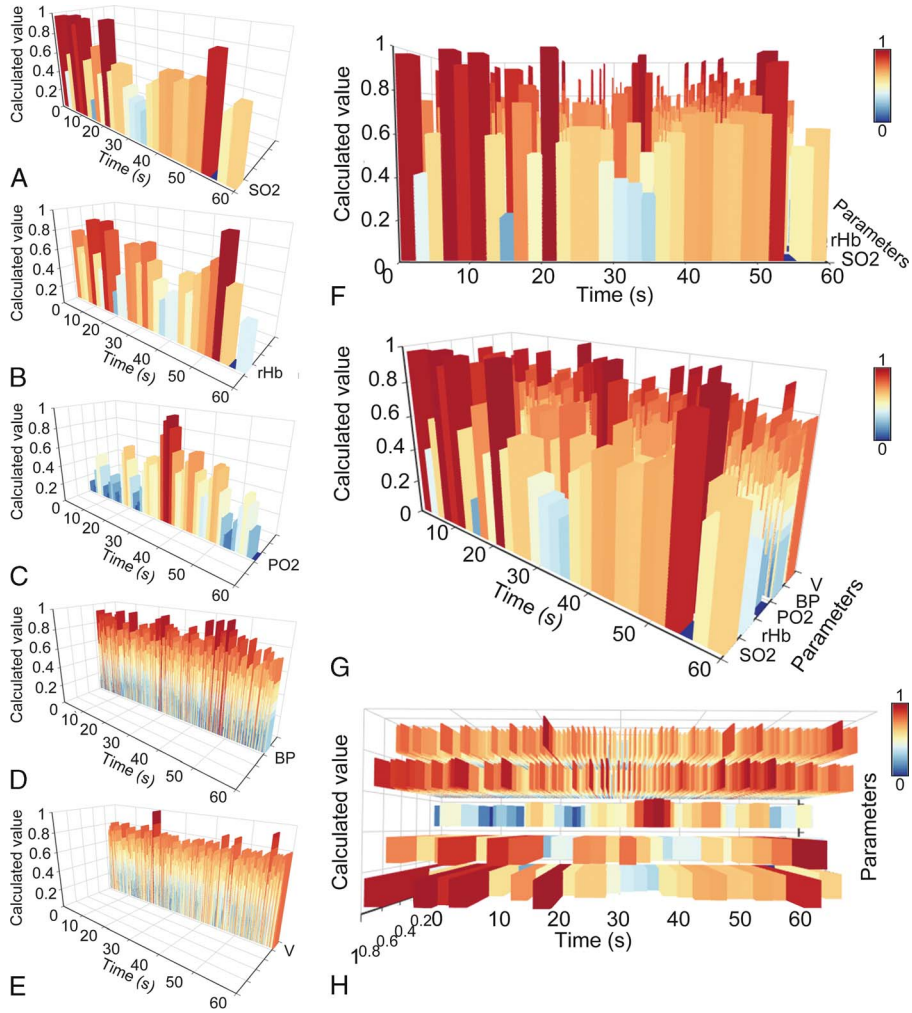

FIGURE 5. Three-dimensional module of pancreatic microcirculation profiles. The continuous pancreatic microcirculatory oxygen and microhemodynamic data were captured and processed. A–E, So_2, rHb, Po_2, blood perfusion, and velocity were set in the coordinates respectively. F–H, The front view, side view, and overlook view of the pancreatic microcirculation profiles were generated by rotation. The front view was shown in F, whereas the side view in G was rotated 45 degrees toward left. The overlook view in H was rotated 90 degrees toward down. Color bar depicts calculated values of pancreatic microcirculatory data set.

TX3 probes could reflect capillary-venous compartment of the microcirculation profiles due to approximately 80% of hemoglobin is located in the capillary and postcapillary of microvascular bed. Monitoring of microcirculatory oxygenation and oxygen delivery-consumption balance could provide oxygen information of pancreatic microcirculation profiles.

For pancreatic microhemodynamics, efforts were made to capture and evaluate pancreatic microcirculatory blood perfusion through several approaches. A line-scanning confocal microscopy approach was established to examine the intraislet blood flow in mice.[13] Taso et al[14] measured pancreatic flow by using noninvasive arterial spin labeling magnetic resonance imaging. Furthermore, weight-adapted ultralow-dose pancreatic perfusion computed tomography had been reported that could obtain the blood perfusion parameters including blood flow, volume, and permeability.[15–17] In the current study, the oscillated microhemodynamics indicated the dynamic changes of pancreatic microvascular vasomotion.[18] Microvascular vasomotion is a specific phenotype of spontaneous oscillation of microvascular tone generated within the vascular wall,[19] which may be synchronized and regulated by neuronal or humoral inputs. The pancreatic vasomotor tone is recognized as an integrated result of the metabolic processes, which in turn regulates the pancreatic microvascular reactivity (vasodilation or vasoconstriction) acting as a specific modulator of pancreatic microcirculatory blood flow.[20] We advanced the algorithm about analyzing pancreatic microcirculatory blood perfusion data set, so that it can perform fast and automatic analysis of a number of microhemodynamic parameters (including the average microvascular blood perfusion, frequency and amplitude of microvascular vasomotion, data not shown). This was due to the built-in computer with home-made combinations of image processing and visualization algorithms (raw data preprocessing and computational transforming, etc).

As for the microcirculation profiles, microvascular blood perfusion and distribution are physiological responses that match oxygen delivery to metabolic demand of tissues.[21] Although heterogeneous, there may be an internal connection between pancreatic microcirculatory blood perfusion and oxygen distribution. According to Fick principle, the amount of transported oxygen (V_Q) is calculated as Q ($C_A - C_V$), where Q is microcirculatory

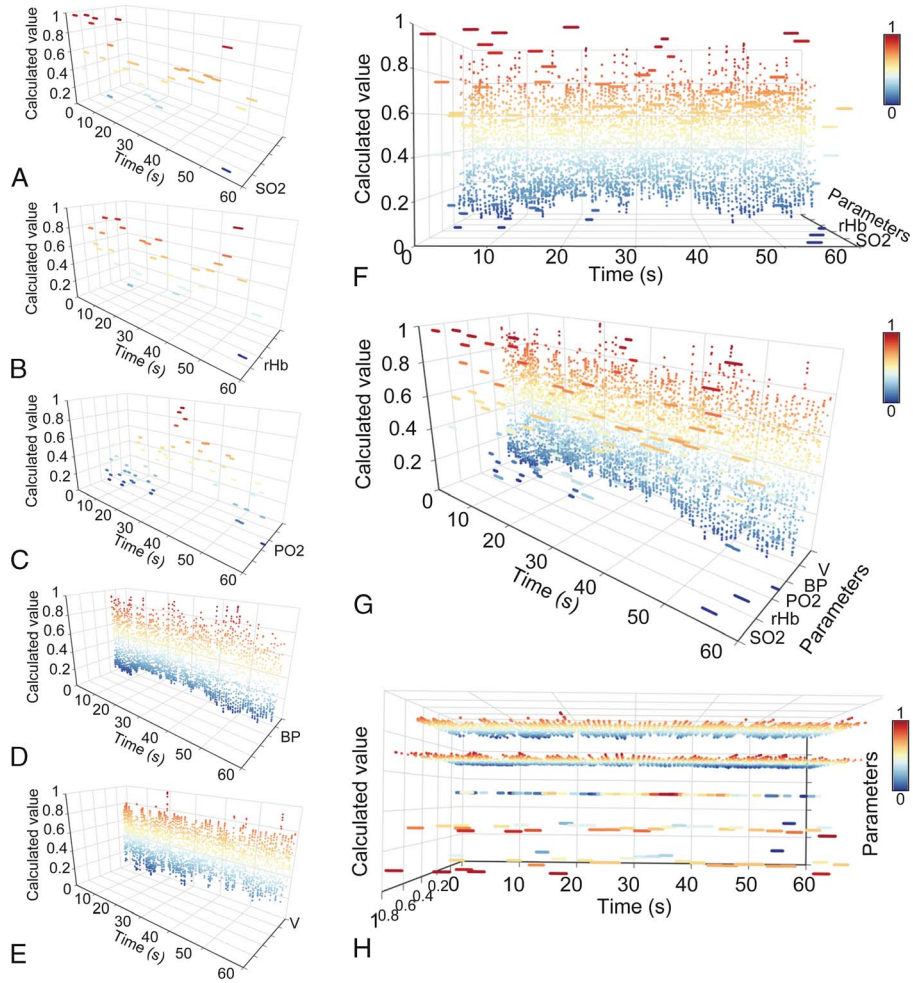

FIGURE 6. Three-dimensional distribution module of pancreatic microcirculation profiles. A–E, Construction of distribution module of pancreatic microcirculation profiles. Separated pancreatic microcirculatory oxygen and microhemodynamic data. F–H, Integrated 3-D distribution module of pancreatic microcirculation profiles. The front view, side view, and overlook view of the distribution module were generated by rotation. The front view was shown in F, whereas side view in G was rotated 45 degrees toward left. The overlook view in H was rotated 90 degrees toward down. Color scattered dots represent calculated values.

blood flow, and C_A and C_V represent arterial and venous O_2 concentration, respectively. It has been reported that the average resting Po_2 was approximately 25 mm Hg with relatively little variation.[22] In our current data, pancreatic microcirculatory Po_2 was linearly related to resting blood flow (data not shown), and no regional differences in blood flow or oxygen were found in pancreas consistent with a previous report,[23] which means that we could use the average oxygen data to represent the oxygen status of pancreatic microcirculation profiles. Furthermore, microcirculation has been shown to represent an important mechanism for tissue oxygenation through microvascular oscillation (so called vasomotion).[19,24] Theoretical modeling of microcirculatory oscillation also suggested that these oscillations might ensure adequate oxygen delivery to all tissues.[25] Our computer algorithm–based pancreatic microcirculation profiles support mega data and longitudinal monitoring of microcirculatory alterations, thereby enabling the proposed opportunity to confirm the link between microcirculatory blood perfusion-oxygen and related physiological performance of pancreas tissue.

In summary, we established the multimodal device and computer algorithm–based pancreatic microcirculation profile monitoring platform and 3-D modules for visualizing integrated pancreatic microcirculatory oxygen and microhemodynamic data sets. Our method provides a useful informative tool and paves the way for the further research concerning pancreatic microcirculation profiles.

REFERENCES

1. Popel AS, Johnson PC. Microcirculation and hemorheology. *Annu Rev Fluid Mech*. 2005;37:43–69.
2. Liu M, Zhang X, Li A, et al. Insulin treatment restores islet microvascular vasomotion function in diabetic mice. *J Diabetes*. 2017;9:958–971.
3. Pan Z, Feng L, Long H, et al. Effects of local pancreatic renin-angiotensin system on the microcirculation of rat with severe acute pancreatitis. *Korean J Physiol Pharmacol*. 2015;19:299–307.
4. Liu LT, Li Y, Fan LQ, et al. Effect of vascular bradykinin on pancreatic microcirculation and hemorheology in rats with severe acute pancreatitis. *Eur Rev Med Pharmacol Sci*. 2015;19:2646–2650.
5. Schmidt J, Ryschich E, Maksan SM, et al. Influence of gastrointestinal hormones on tumor microcirculation of experimental pancreatic cancer in the rat. *Dig Surg*. 2000;17:250–255.

6. Lytras D, Leontara V, Kefala M, et al. Microvessel landscape assessment in pancreatic ductal adenocarcinoma: unclear value of targeting endoglin (CD105) as prognostic factor of clinical outcome. *Pancreas*. 2015;44: 87–92.
7. Liu M, Zhang X, Wang B, et al. Functional status of microvascular vasomotion is impaired in spontaneously hypertensive rat. *Sci Rep*. 2017; 7:17080.
8. Premont RT, Reynolds JD, Zhang R, et al. Role of nitric oxide carried by hemoglobin in cardiovascular physiology: developments on a three-gas respiratory cycle. *Circ Res*. 2020;126:129–158.
9. Meglinsky IV, Matcher SJ. Modelling the sampling volume for skin blood oxygenation measurements. *Med Biol Eng Comput*. 2001;39: 44–50.
10. Aksoy S, Haralick RM. Feature normalization and likelihood-based similarity measures for image retrieval. *Pattern Recogn Lett*. 2001;22: 563–582.
11. Gorczyca J, Tomaszewski KA, Henry BM, et al. The vascular microarchitecture of the human fetal pancreas: a corrosion casting and scanning electron microscopy study. *Pancreas*. 2017;46:124–130.
12. Samraj RS, Nicolas L. Near infrared spectroscopy (NIRS) derived tissue oxygenation in critical illness. *Clin Invest Med*. 2015;38:E285–E295.
13. Nyman LR, Wells KS, Head WS, et al. Real-time, multidimensional in vivo imaging used to investigate blood flow in mouse pancreatic islets. *J Clin Invest*. 2008;118:3790–3797.
14. Taso M, Papadopoulou F, Smith MP, et al. Pancreatic perfusion modulation following glucose stimulation assessed by noninvasive arterial spin labeling (ASL) MRI. *J Magn Reson Imaging*. 2020;51: 854–860.
15. Li P, Deng W, Xue H, et al. Weight-adapted ultra-low-dose pancreatic perfusion CT: radiation dose, image quality, and perfusion parameters. *Abdom Radiol (NY)*. 2019;44:2196–2204.
16. Li HO, Guo J, Sun C, et al. Assessment of pancreatic adenocarcinoma: use of low-dose whole pancreatic CT perfusion and individualized dual-energy CT scanning. *J Med Imaging Radiat Oncol*. 2015;59:590–598.
17. Tan Z, Miao Q, Li X, et al. The primary study of low-dose pancreas perfusion by 640- slice helical CT: a whole-organ perfusion. *Springerplus*. 2015;4:192.
18. Liu M, Zhang X, Li B, et al. Laser Doppler: a tool for measuring pancreatic islet microvascular vasomotion in vivo. *J Vis Exp*. 2018;133:56028.
19. Nilsson H, Aalkjaer C. Vasomotion: mechanisms and physiological importance. *Mol Interv*. 2003;3:79–89, 51.
20. Vollmar B, Menger MD. Microcirculatory dysfunction in acute pancreatitis. A new concept of pathogenesis involving vasomotion-associated arteriolar constriction and dilation. *Pancreatology*. 2003;3:181–190.
21. Diesen DL, Hess DT, Stamler JS. Hypoxic vasodilation by red blood cells: evidence for an s-nitrosothiol-based signal. *Circ Res*. 2008;103:545–553.
22. Granger DN, Holm L, Kvietys P. The gastrointestinal circulation: physiology and pathophysiology. *Compr Physiol*. 2015;5:1541–1583.
23. Harper SL, Pitts VH, Granger DN, et al. Pancreatic tissue oxygenation during secretory stimulation. *Am J Physiol*. 1986;250:G316–G322.
24. Goldman D, Popel AS. A computational study of the effect of vasomotion on oxygen transport from capillary networks. *J Theor Biol*. 2001;209: 189–199.
25. Kislukhin VV. Regulation of oxygen consumption by vasomotion. *Math Biosci*. 2004;191:101–108.